ISSN 2472-1972

Novel *CYP19A1* Mutations Extend the Genotype-Phenotype Correlation and Reveal the Impact on Ovarian Function

Valiyaparambil Pavithran Praveen,[1] Asmahane Ladjouze,[2] Kay-Sara Sauter,[3] Annie Pulickal,[1] Efstathios Katharopoulos,[3] Mafalda Trippel,[4] Aurel Perren,[4] Amit V. Pandey,[3] and Christa E. Flück[3]

[1]Department of Endocrinology, Amrita Institute of Medical Sciences, Kochi, Kerala 682041, India; [2]Department of Pediatrics, CHU Bab El Oued, 16000, Algiers, Algeria; [3]Department of Pediatrics, Division of Pediatric Endocrinology, Diabetology and Metabolism University Children's Hospital Bern, Switzerland, and Department of Biomedical Research, University of Bern, 3010 Bern, Switzerland; and [4]Institute of Pathology, University of Bern, 3010 Bern, Switzerland.

ORCiD number: 0000-0002-4568-5504 (C. E. Flück).

Context: The steroidogenic enzyme aromatase (CYP19A1) is required for estrogen biosynthesis from androgen precursors in the ovary and extragonadal tissues. The role of aromatase, and thus estrogens, is best illustrated by genetic variations of the *CYP19A1* gene leading to aromatase deficiency or excess.

Objective: The objective of this work is to characterize novel *CYP19A1* variants.

Design, setting, and patients: Variants causing aromatase deficiency were suspected in four 46,XX children of African and Indian origin by careful clinical phenotyping. Sequencing of the *CYP19A1* gene identified novel variants. Minigene experiments, aromatase activity assay, and computational, and histological analysis were used to characterize the variants.

Main outcome measure and results: *CYP19A1* variants were found in all patients: a deletion in intron 9 leading to p.P423_H503del, a delins variant at p.P154, and point variants p.V161D, p.R264C, p.R375C. Except for R264C, all variants showed a loss of function. Protein structure and dynamics studies were in line with functional assays. The 2 female patients with delins variants manifested with ambiguous genitalia at birth. Histologic investigation revealed normal ovarian tissue on one side and a streak gonad on the other. Two female patients presented with abnormal pubertal development and polycystic ovaries.

Conclusion: In girls, aromatase deficiency usually manifests at birth, but diagnosis may also be made because of abnormal pubertal development or ovarian torsion due to (poly)cystic ovaries. The ovary harboring *CYP19A1* variants may present as streak gonad or appears normal at birth, but is then at very high risk to produce cysts with aging and is therefore prone to ovarian torsion.

Key Words: aromatase deficiency, CYP19A1, disorder of sexual development, virilization, estrogen synthesis, hyperandrogenism

Abbreviations: CAH, congenital adrenal hyperplasia; FSH, follicle-stimulating hormone; LH, luteinizing hormone; MAF, minor allele frequency

Received 10 January 2020
Accepted 4 March 2020
First Published Online 10 March 2020
Corrected and Typeset 27 March 2020

The CYP19A1 gene encodes the steroidogenic enzyme aromatase on chromosome 15q21.2 (OMIM 107910; RefSeq NM_000103.3). It spans over 123 kb and consists of 9 coding exons (spanning over 30 kb, exons 2-10). For the *CYP19A1* gene, a large number of alternative first exons and 9 different transcriptional start sites with individual promoters have been described [1, 2]. Several tissues use their specific promoters leading to a very complex tissue-specific regulation of CYP19A1 expression. Metabolic activities of aromatase include the biosynthesis of estrone from androstenedione, estriol from 16-hydroxytestosterone, and 17β-estradiol from testosterone [3]. Of these, androstenedione and testosterone are the common physiological steroid substrates of aromatase [3-5]. Recently 16β-OH-androstenedione was also reported to be a substrate for aromatase [6]. Although the human ovary is the principal site of estrogen production, even the testis produces estrogens, and extragonadal synthesis occurs from circulating C19 steroids in bone, breast, brain, adipose, and other tissues through aromatase expressed in these tissues. The role of aromatase and thus estrogens for human biology is best illustrated in disease states, both deficiency and excess.

Aromatase deficiency (OMIM 613546) is a rare, autosomal recessive disorder that was first described in 1991 by Shozu et al in a mother who experienced virilisation during pregnancy due to a 46,XX fetus with aromatase deficiency that presented with severe virilization of the external genitalia at birth [7]. Meanwhile, about 50 cases of aromatase deficiency due to variants in *CYP19A1* have been reported, both in female and male patients (Table 1 and Fig.1) [7-42]. During pregnancy, aromatase deficiency of the fetus typically manifests in the pregnant mother by progressive virilization due to the inability of the placenta to aromatize androgens derived from the fetal adrenals. These androgens also virilize the 46,XX fetus. During infancy and childhood, aromatase deficiency may go unnoticed, although, in some girls, abdominal problems may be seen due to ovarian cysts caused by a lack of feedback regulation of estrogens to the hypothalamic-pituitary-gonadal axis [34]. At puberty, girls without aromatase activity are not able to produce estrogens from androgen precursors for pubertal development, for example, breast and uterine development. Young men with aromatase deficiency usually present in the second decade of life with low bone mass and unfused epiphyses leading to persistent growth into adulthood with extremely tall stature [43]. In addition, aromatase deficiency is reported to cause disturbances of the lipid profile and insulin sensitivity (eg, metabolic syndrome), and it may also cause male infertility and affect bone quality.

Aromatase excess (OMIM 139300) has been found in a few, mostly familial cases of gynecomastia associated with accelerated growth and bone maturation due to excessive peripheral estrogen production. The main causes of aromatase excess include chromosomal rearrangements altering regulatory elements of the *CYP19A1* gene expression or a higher expression of an alternative first exon enhancing *CYP19A1* transcription [44, 45]. By contrast, aromatase deficiency is almost exclusively caused by variants altering the coding sequence of the *CYP19A1* gene, such as point mutations, deletions, and insertions, or splicing mutations (Table 1 and Fig. 1).

In this study, we describe several novel variants in *CYP19A1*. A homozygote splice-site deletion in the *CYP19A1* gene was found in an African 46,XX neonate presenting with typical clinical manifestations during pregnancy and at birth. An indel variant in exon 5, together with the c.–41C>T variant in the *CYP19A1* promoter that had been described earlier, was found in an Indian 46,XX child presenting with an unsolved disorder of sex development at age 3 years. Novel point variants were identified in 2 more unrelated adolescent girls in India who presented with poor breast development and polycystic ovaries. To address the impact of the novel *CYP19A1* variants manifesting at different time points of sex development and originating from diverse populations, we performed genetic, functional, and structural studies and compared the findings of novel variants in the *CYP19A1* gene with the published literature.

Table 1. Summary of all reported human CYP19A1/aromatase mutations and their characteristics

No. of patients	Familial	Consanguinity	Mutation Allele 1	Mutation Allele 2	Karyotype	Sex of rearing	Age at Presentation	Phenotype	Virilization of Baby at Birth	Virilization of Mother	Spontaneous Puberty	Ovary/Testis Phenotype	Functional Testing	Ref.
2	Yes	NK	M85R	c.629-2G>A	46,XX	F	Birth	Ambiguous genitalia at birth, puberty absent and bone age delayed, virilizing signs at pubertal age	Yes	NK	NK	NK	M85R: no activity	(8)
2	Yes	Likely	R115X	R115X	46,XX	M + F	14/8	P1 (M): At 14 y, undescended testes and hypospadias, presence of ovaries with cysts and small uterus. P2 (F): At 8 y, 1 cm phallus, 2 urogenital openings, pubic pilosity	Yes (Prader III in P1 and II in P2)	No	Yes	Histo P1: ovarian follicle cysts	ND	(9)
2	Yes	Yes	W141X	P1: W141X; P2: missing allele/ deletion	46,XX	F	2/5	Hypertrophic clitoris and prepuce with single urogenital opening; low estradiol, elevated LH and FSH	Yes (Prader IV)	Yes	No	Normal at presentation	ND	(10)
2	No	No	E210K	E210K	46,XX	F	Birth	P1: Ambiguous genitalia at birth, spontaneous pubertal development Tanner 4 with virilization signs; menarche at 12 y. P3: Clitorial enlargement with complete labial fusion and urogenital sinus with single phalloscrotal opening; gonads nonpalpable. Spontaneous puberty starting at 9 y, Tanner 3 at 12 y with signs of virilization and elevated gonadotropins	Yes (Prader II in P1; IV in P3)	No	Yes	Multiple cysts in both ovaries at age 18 y (P1) and at 9 y (P3)	ND	(11)
1	No	No	E210K	E210K	46,XY	M	25	29 y, tall, eunuchoid habitus, cryptorchidism, bone pain, metabolic syndrome	NA	NK	Yes	Histo: hypotrophic seminiferous tubules with mature Sertoli cells. Germ cell depletion without spermatogenic development. Scarce, mature Leydig cells in small groups.	ND	(12)

Table 1. Continued

No. of patients	Familial	Consanguinity	Mutation Allele 1	Mutation Allele 2	Karyotype	Sex of rearing	Age at Presentation	Phenotype	Virilization of Baby at Birth	Virilization of Mother	Spontaneous Puberty	Ovary/Testis Phenotype	Functional Testing	Ref.
1	No	No	E210K	c.1235delA	46,XX	F	Birth	Ambiguous genitalia and virilization (Prader V), PCOS in childhood; spontaneous breast development at age 8 y	Yes (Prader V)	Yes	Yes (partial)	Large ovarian follicles at 5 mo; Histo: normal stroma, numerous follicles. At 7.7 y: increased size of uterus with multiple ovarian cysts	c.1235delA: no activity	(11) (13-15)
1	No	No	E210K	Y81C	46,XX	M to F	Birth	Phallic enlargement, hypospadias, nonpalpable gonads. Delayed bone age at 6 y	Yes (Prader IV)	Yes	NA	Bilateral ovaries with cysts	ND	(11)
1	No	No	R192C	R192C	46,XX	F	Birth	Ambiguous genitalia, 2 cm phallus	Yes (Prader IV)	Yes	NA	Normal by ultrasound at years 3	ND	(11)
1	No	No	R192C	R457X	46,XX	F	Birth	Ambiguous genitalia, 1 cm phallus and complete labial fusion. Single phalloscrotal opening. No gonads palpable.	Yes	No	Yes	At 10 y, enlarged ovaries by ultrasound	ND	(11)
2	Yes	Yes	R192H	R192H	46,XX and 46,XY	F + M	F at birth; M at 15 mo	F: Clitoral hypertrophy and labial fusion; M: hypospadia and cryptorchidism	F: yes (Prader IV)	No	NK	Histo of ovary at 1 year: normal.	19% of WT	(1)
1	No	Yes	R365Q	R365Q	46,XY	M	28	28 y, continuous growth and unfused epiphysis, infertility, skeletal pain, metabolic syndrome	NA	NK	Yes	Histo: hypospermatogenesis and germ cell arrest	0.4% of WT	(16)
1	No	Likely	V370M	V370M	46,XX	F	Birth	Ambiguous genitalia (small phallic structure without hypospadias); not palpable gonads. Urogenital sinus	Yes (Prader V)	Yes	NA	Ovaries not visualized at birth	ND	(17)
2	Yes	Yes	R375C	R375C	46,XX and 46,XY	F + M	Birth	P1, 46,XX, F, 28 y: DSD at birth, sexual infantilism and virilization, PCOS, tall stature. P2, 46,XY, M, 24 y: tall, osteopenia, delayed bone maturation, eunuchoid, macroorchidism	Yes (P1)	Yes	No in P1 (F), yes in P2 (M)	Histo: ovaries with PCOS phenotype	0.2% of WT	(18)
2	Yes	Yes	R375H	R375H	46,XY	M	27	Bone pain and recurrent forearm fractures, progressive overgrowth	NA	NK	Yes	Borderline sperm count and motility	ND	(19)
1	No	No	R375H	M127R	46,XY	M	25	Continuing linear growth, eunuchoid body habitus, adiposity, and diffuse bone pain	NA	NK	Yes	Histo: hypospermatogenesis	R375H: 7% of WT; M127R: 0%	(20)
1	No	No	R435C	R435C	46,XX	F	Birth	Ambiguous genitalia; sexual infantilism, PCO	Yes (Prader IV)	Yes	Yes, partial	Bilateral cystic ovaries at age 13.5 y	1.5% of WT	(21)

Table 1. Continued

No. of patients	Familial	Consanguinity	Mutation Allele 1	Mutation Allele 2	Karyotype	Sex of rearing	Age at Presentation	Phenotype	Virilization of Baby at Birth	Virilization of Mother	Spontaneous Puberty	Ovary/Testis Phenotype	Functional Testing	Ref.
2	Yes	Yes	F234del	F234del	46,XX	M + F	Birth	P1, m: Ambiguous genitalia (phallic enlargement and hypospadia). Gynecomastia at puberty caused gonadectomy. P2, F: Ambiguous genitalia. 2 cm phallus, partial labial fusion.	Yes (Prader IV)	Yes	Yes	Histo: cystic ovaries	19% of WT	(21)
1	Yes	Yes	c.452-621-c.628 + 803del	c.452-621-c.628 + 803del	46,XX	F	Birth	Labial fusion, excess of clitoral skin	Yes	Yes	No	Small ovaries observed with MRI	0%	(21)
1	No	NK	C437Y	R435C	46,XX	F	Birth	Ambiguous genitalia at birth; 14 y: primary amenorrhea, no breast development, enlarged clitoris, pubic hair Tanner stage III, sexual infantilism, PCO	Yes	Only acne	No	Multiple bilateral cysts	C437Y: 0% of WT R435C: 1.1% of WT	(22, 23)
1	No	No	L451P	Y81C	46,XY	M	24	Eunuchoid proportions, bilateral genua valga, incomplete fused epiphyses, osteopenia	NA	No	Yes	Testes of normal size and consistency	L451P: 3.1% of WT Y81C:14.3% of WT	(24)
1	NK	NK	R457X	R457X	46,XX	F	NK	F, virilization	Yes	NK	NK	NK	ND	(25)
1	No	NK	N411S	c.–41C>T	46,XX	F	Birth	At birth ambiguous genitalia, clitoral hypertrophy, thin dividing wall between urethral opening and a normal vaginal introitus with a hymen altus	Yes	Yes	NA	Normal by ultrasound	N411S: 0% of WT c.-41C>T: 50% of WT	(26)
1	No	Yes	c.629-1453_744-486_del	c.629-1453_744-486_del	46,XX	M + F	Birth	At 1 mo: ambiguous genitalia, gonads not palpable, phallus 1 cm, uterus by ultrasound	Yes (Prader III)	No	NA	Small ovaries by ultrasound	ND	(27)
1	No	Yes	c.1263 + 1G>T	c.1263 + 1G>T	46,XX	M	Birth	Ambiguous genitalia of unknown cause at birth. At 21 y: undescended testes, hypoplastic scrotum, hypoplastic uterus	Yes (Prader V)	No	Abnormal	Histo: streak gonads	ND	(28)
1	No	Yes	c.469C_del	c.469C_del	46,XY	M	Birth	Investigated after birth because of severe maternal virilization. Found low estrogen levels, high androstenedione, normal free testosterone.	NA	Yes	NA	Normal	ND	(29)
1	No	Yes	c.264G_del	c.1036_1037ins 23bp	46,XX	F	Birth	Ambiguous genitalia, 3 cm clitoromegaly; PCOS later	Yes (Prader IV)	Yes	NA	Large ovaries with cysts	c.264G_del < 0.3% of WT; 23bp_del < 0.3% of WT	(30)

Table 1. Continued

No. of patients	Familial	Consanguinity	Mutation Allele 1	Mutation Allele 2	Karyotype	Sex of rearing	Age at Presentation	Phenotype	Virilization of Baby at Birth	Virilization of Mother	Spontaneous Puberty	Ovary/Testis Phenotype	Functional Testing	Ref.
1	No	Yes	Ala306_Ser314_dup	Ala306_Ser314_dup (likely)	46,XX	F	Birth	At birth ambiguous genitalia. Lack of pubertal development. Streak ovaries. At 32 y, osteopenia and fracture, tall stature, central obesity, borderline hypertension, impaired fasting glucose	Yes (Prader III)	NK	No	Streak ovaries	ND	(31)
1	No	No	c.1263 + 5G>A	c.1263 + 5G>A	46,XX	F	4	At 4, labioscrotal fusion, 1.5 cm clitoromegaly, perineal urethra. At 13.5 y, delayed bone age, small uterus, follicular cysts in ovaries.	Yes	No	Abnormal (B1, P4)	PCOS	ND	(32, 42)
1	No	Yes	c.743 + 2T>C	c.743 + 2T>C	46,XX	F	Birth	At birth: ambiguous genitalia, enlarged phallus, gonads not palpable	Yes (Prader IV-V)	Yes	NA	ND	0.3% of WT	(7, 33)
1	No	No	V445X	c.296 + 1G>A	46,XX	F	Birth	At birth: masculine-appearing external genitalia, enlarged phallus, complete fusion of posterior labioscrotal folds	Yes (Prader V)	Yes	Yes (Tanner 4)	At birth: slightly enlarged ovaries. At 2 y: enlarged ovaries with several cysts, fallopian tubes and uterus normal in appearance, histopathology showed many normal-appearing large tertiary follicles with an oocyte within a cumulus oophorus projecting into antrum.	ND	(34, 35)
2	Yes	Yes	c.469C_del	c.469C_del	46,XY and 46,XX	M + F	16 (M	P1 (M): 16 y, no gynecomastia or other abnormalities, open epiphyses, congenital hearing loss of 85%, delayed bone age	NA and NK (F)	No	M: yes and F: no	Normal by clinical exam	ND	(36)
1	No	Yes	c.629-3C>A–frameshift and stop codon 8 nt after exon 5	c.629-3C>A–frameshift and stop codon 8 nt after exon 5	46,XY	M	27	Normal sex characteristics, spontaneous erections sufficient for intercourse, genua valga, kyphoscoliosis, pectus carinatus. Retarded bone maturation. Abnormal glucose and lipid metabolism.	NA	Yes	Yes	Below threshold sperm count (1 mL/mL), 100% immotile spermatozoa. Oligoazoospermia	ND	(37)
1	No	NK	c.311-334_del	c.1263 + 1G>T → Y361X	46,XY	M	27	At 27 y, height 193 cm, eunuchoid, unfused epiphyses, osteopenia, increase fasting insulin, mild astenozoospermia and history of right cryptorchidism	NA	NK	Yes	History of cryptorchidism. Borderline FSH and inhibin B at age 27 y	ND	(38)

Table 1. Continued

No. of patients	Familial	Consanguinity	Mutation Allele 1	Mutation Allele 2	Karyotype	Sex of rearing	Age at Presentation	Phenotype	Virilization of Baby at Birth	Virilization of Mother	Spontaneous Puberty	Ovary/Testis Phenotype	Functional Testing	Ref.
1	No	Yes	c.744-2A>G	c.744-2A>G	46,XX	F	Birth	Ambiguous genitalia at birth; 19 mo: gonads not palpable, penis-like phallus 1.5 cm, single penoscrotal urethral opening, labioscrotal fusion defect	Yes (Prader IV)	Yes	NA	Very small ovaries by ultrasound	ND	(39)
1	NK	NK	c.1058insT	c.1058insT	46,XY	M	26	190 cm tall, hypertension, hyperuricemia, hypercholesterolemia	NA	NK	Yes	NK	ND	(40)
3	Yes	Yes	c.568insC → L190P leading to S199X	c.568insC → L190P leading to S199X	46,XX	F	Birth	Clitoromegaly, partial to complete labial fusion	Yes (Prader II-III)	Yes	NA	Hypoplastic ovaries by imaging studies	ND	(41)

Abbreviations: DSD, disorder of sex development; F, female; FSH, follicle-stimulating hormone; LH, luteinizing hormone; M, male; MRI, magnetic resonance imaging; NA, not applicable; ND, not determined; NK, not known; P1, patient 1; P2, patient 2 etc; PCOS, polycystic ovary syndrome; WT, wild-type.

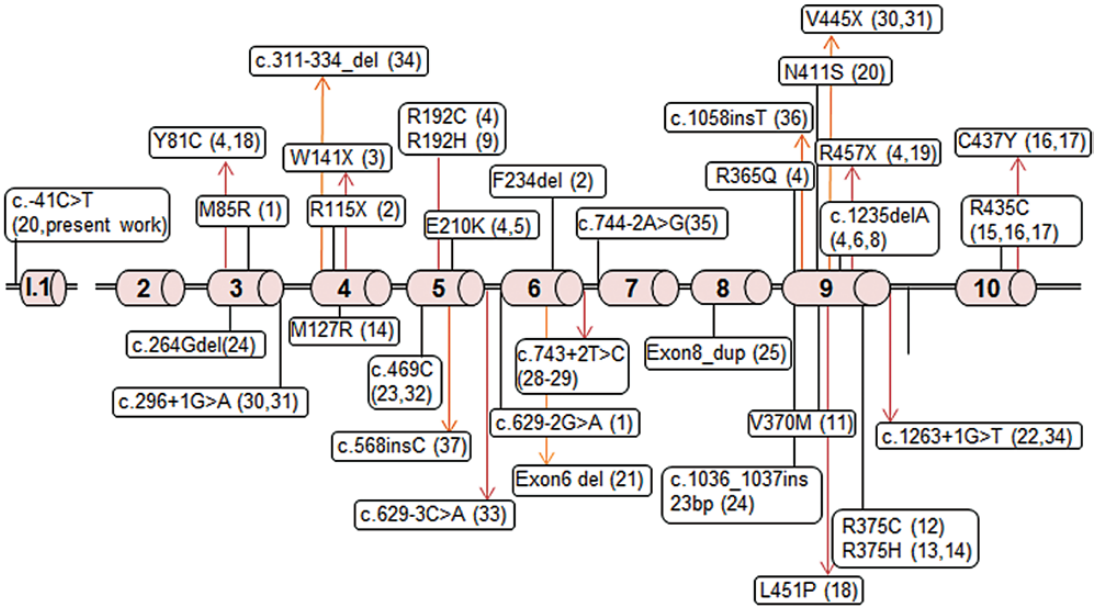

Figure 1. Localization of reported *CYP19A1* variants. The coding exons 2 to 10 and the alternative exon I.1 of the aromatase *CYP19A1* gene are shown.

1. Case Reports, Materials, and Methods

A. Case Reports

Family 1. An 8-day-old newborn was referred to the clinic of A.L. for assessment of ambiguous genitalia. The infant was the seventh child of second-degree consanguineous African parents. The first child was stillborn (Fig. 2). There was maternal virilization during the second pregnancy and the newborn who was declared "male," died on the first day of life (with no further details available). After delivery, signs of virilization slowly decreased in the mother, and she subsequently gave birth to 4 healthy sons without suffering from virilization again during these pregnancies. However, during the seventh pregnancy, the mother, age 36 years, again developed progressive signs of virilization from 12th week of gestation, with facial and abdominal hirsutism, facial acne, clitoral hypertrophy, and deepening of the voice. No drugs or environmental toxins were suspected of influencing the pregnancy. Biochemical workup of the mother revealed marked hyperandrogenism with high testosterone levels (eg, 45.1 nmol/L at 32/40 weeks of pregnancy, normal range is 2.2-10.7 nmol/L). Ultrasound and magnetic resonance imaging studies after delivery revealed enlarged ovaries containing multiple follicles consistent with polycystic ovaries. However, the signs of virilization decreased slowly after birth, and serum testosterone levels normalized within 1 month.

The baby was born at term by spontaneous vaginal delivery. Birth weight, length, and head circumference were normal (3500 g/50 cm/35 cm). Neonatal adaptation was also normal, but the baby had ambiguous genitalia without presenting other dysmorphic features. Genital examination showed a 1.5 cm cliterophallus with a single meatus opening at the base of the genital tubercle and a complete posterior labial fusion (Prader IV). The genital folds were scrotalized, and no gonads were palpable (Fig. 3). Pelvic ultrasound showed a uterus, whereas the gonads were not visible. Karyotype was 46,XX. Biochemical workup revealed normal electrolytes, 17α-hydroxyprogesterone, cortisol, and renin levels, ruling out classic 21-hydroxylase deficiency with congenital adrenal hyperplasia (CAH) (Table 2). Testosterone levels were slightly elevated at birth but decreased to normal levels by 1 month, whereas other androgen levels were within reference ranges. Estradiol levels were very low (Table 2). Follow-up revealed that the patient did not have any distress as

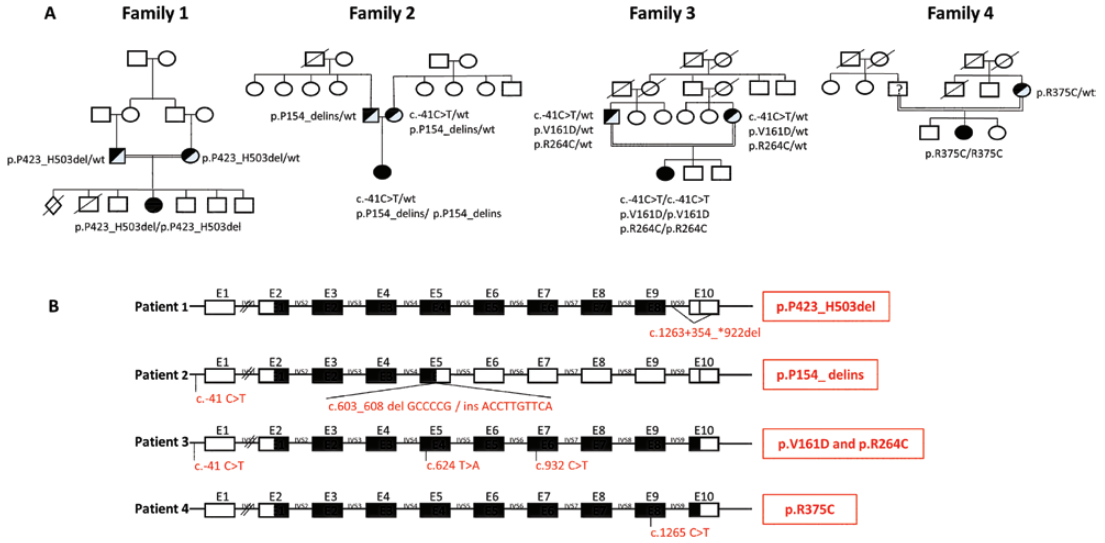

Figure 2. Genetic characterization of 4 patients harboring novel *CYP19A1* variants. A, Family pedigrees show consanguinity in 3 families. B, Diagram showing localization and specific variations in the *CYP19A1* gene with respect to exon-intron boundaries. Black-filled exon rectangles show exons that are translated into RNA/protein sequences despite the genetic variations.

seen in cortisol deficiency. Thus virilization of the 46,XX baby with concurrent virilization of the mother during pregnancy suggested aromatase deficiency in the child.

Patient 2. This 46,XX infant was referred to the clinic of V.P.P. for workup of ambiguous genitalia at age 3 years. She was the only child of nonconsanguineous Indian parents and was noted to have a phallic structure with absent gonads at birth. There was no history of maternal virilization or hirsutism during pregnancy. Evaluation elsewhere had ruled out CAH. Karyotype was 46,XX, and laparoscopy had been performed at age 8 months and revealed a uterus and fallopian tubes. Unilateral gonad biopsy was suggestive of ovarian tissue. At age 3 years, she presented with a well-formed phallus with a single opening at the tip with good prepucial skin and fused labioscrotal folds with rugosity (Prader IV). Gonads were not palpable. Biochemical workup revealed normal cortisol response to an adrenocorticotropin stimulation test (60 minutes, 745 nmol/L), normal 17-hydroxyprogesterone, undetectable testosterone, elevated follicle-stimulating hormone (FSH), and prepubertal luteinizing hormone (LH) (Table 2). A 100 cell count karyotype was repeated, which again revealed only 46,XX cell lines. Laparoscopy was also repeated and confirmed earlier findings; gonadal biopsy from the other side revealed primordial follicles with ovarian stroma. Because of normal stimulated serum cortisol and 17-hydroxyprogesterone, P450 oxidoreductase deficiency (PORD) was considered less likely and aromatase deficiency was suspected.

Patient 3. Patient 3, from India, presented at age 14 years with an acute abdomen due to ovarian torsion. She was the second child of consanguineous parents (Fig. 2). Past medical history was suggestive for some maternal virilization during pregnancy, but at birth, the girl was recorded to be healthy, although retrospectively the prominence of the clitoris was present since birth. Pubertal development started at around age 11 years with pubic and axillary hair, and voice change was noted; breast development started after age 12.5 years, and growth of facial hair in the past 6 months was noted. Physical exam revealed a weight of 40.6 kg (P10), height 160 cm (P50), blood pressure 90/50 mm Hg, Ferriman Gallway Score 4, and Tanner stage B3/P4/A3. Exam of the external genitalia revealed a slightly enlarged clitoris (> 1 cm). Biochemical workup showed elevated LH, FSH, and testosterone with rather low estradiol (Table 2). Ultrasound and laparoscopy revealed polycystic ovaries on both sides with torsion of the left ovary.

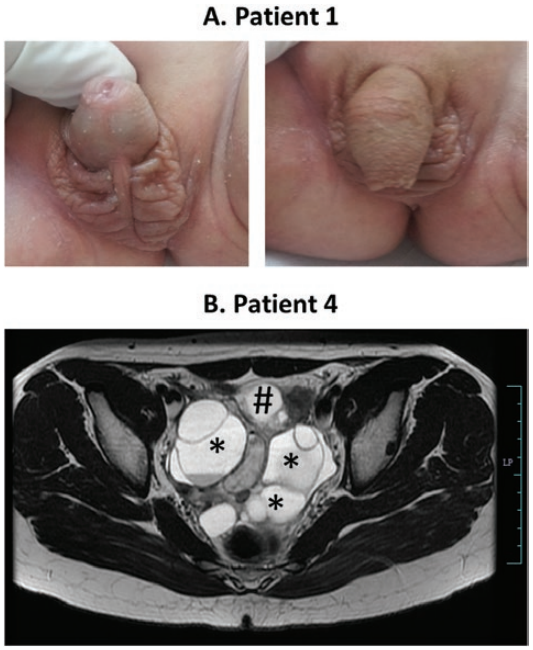

Figure 3. Phenotype of girls with *CYP19A1* mutations. A, Picture of the ambiguous genitalia at birth found in the 46,XX disorder of sex development index patient 1. Note the phallus-like tubercle with a single meatus opening at the base and the complete labioscrotal fusion (Prader IV). The photograph is shown with the permission of the parents. B, Magnetic resonance imaging of the pelvis in patient 4 at age 14 years showing a large, multiloculated, cystic mass (6.8 × 9.6 × 6.5 cm) involving bilateral adnexa (*), displacing the uterus (#) anteriorly and inferiorly. Few of the cysts are showing hemorrhage. Both ovaries cannot be separately visualized.

Patient 4. Patient 4, from India, born to consanguineous parents, presented at age 14 years for abdominal pain and oligomenorrhea. No maternal virilization was reported during pregnancy. The girl likely had atypical genitalia at birth, but this was not recorded. Pubertal development started at around age 10 to 11 years with menarche at around 12 years. Breast development was poor, and clitoromegaly was claimed. At presentation, her weight was 50 kg (P50), height 155 cm (P25), and blood pressure was 90/60 mm Hg. No skeletal anomalies were found, and Tanner stage was B3P4A3. The genital exam showed a clitoromegaly of 20 mm, a common urogenital sinus, and posterior labial fusion. Ultrasound and magnetic resonance imaging revealed enlarged polycystic ovaries (Fig. 3). Laboratory findings were abnormal for elevated LH, FSH, and testosterone, whereas estradiol was not detectable (Table 2).

B. Genetic Studies

Genetic studies of rare steroid disorders were approved by the cantonal ethics' commission of Bern, Switzerland. Written informed consent for the genetic studies was obtained from parents and teenage minors. DNA was extracted from blood samples of the patient and both parents as available. The *CYP19A1* gene (NM_000103.3 or NG_007982.1) was sequenced from genomic DNA using a candidate exon-by-exon approach, as previously described [1]. Additional primers were used to characterize the deletion found at the boundary of exon/intron 9 and the deletion/insertion in exon 5; these primer sequences are available on request.

For the minigene experiment for genetic workup of patient 1, the wild-type (wt) and variant genomic *CYP19A1* sequence comprising exon 9 to exon 10 – 3'UTR was cloned in a pcDNA3.1 vector. These vectors were then transiently transfected in HEK293 cells using Lipofectamine 2000 (Invitrogen AG, Life Technologies). Forty-eight hours after transfection,

Table 2. Clinical and biochemical characteristics of four 46,XX patients with aromatase deficiency

							Laboratory Findings							
Pt ID	**Origin**	**Maternal virilization**	**Age at Manifestation/Follow-up**	**Genital Phenotype**	**Pubertal Development (Tanner stage)**	**Ovarian Phenotype**	**T, nmol/L**	**DHEAS, µmol/L**	**4A, nmol/L**	**17OHP, nmol/L**	**Cortisol, nmol/L**	**E2, pmol/L**	**LH, IU/L**	**FSH, IU/L**
1	African	Yes	Birth	Prader IV	NA	NK	**3.41**			**55.9**				
			10 d				**2.03**	**1.34**	**4.85**	11.92	504			
			1 mo				0.19	**0.35**	0.8	3.85	305	< 18		
			4 mo (minipuberty)				**0.38**			1.04				
2	Indian	No	Birth	Atypical genitalia	NA									
			3 y	Prader IV	NA	See Figure 3.	< 0.45			5	745[a]	NM	< 1	**12**
3	Indian	Maybe	14 y	Clitoromegaly	B3/P4/A3	Polycystic ovaries, ovarian torsion	**2.06**	1.93		2.03	648[a]	58.7	**39.9**	**10.98**
4	Indian	Yes	14 y	Clitoromegaly	B3/P4/A3	Polycystic ovaries	**2.6**	3.58		1.38	634[a]	**< 18**	**32**	**37**

Laboratory values outside the normative range are shown in bold.

Abbreviations: 4A, androstenedione; 17OHP, 17α-hydroxyprogesterone; DHEAS, dehydroepiandrosterone-sulfate; E2, estradiol; FSH, follicle-stimulating hormone; LH, luteinizing hormone; NA, not applicable; NK, not known; NM, not measurable; Pt, patient; T, testosterone.

[a]Adrenocorticotropin-stimulated 60-minute values.

doi: 10.1210/jendso/bvaa030 | Journal of the Endocrine Society | 11

total RNA was extracted and reverse transcribed. Finally, transcripts of wt and variant vectors were polymerase chain reaction amplified. Polymerase chain reaction products were run on an agarose gel and visualized, as well as subjected to direct sequencing (Microsynth AG).

C. Analysis of Conservation of Amino Acids of CYP19A1

We used ConSurf analysis to study the evolutionary conservation of amino acids (aa) in CYP19A1 based on structural and phylogenetic relationships between the sequences from different species [46, 47]. All CYP19A1 sequences in the Uniprot database were searched, and the best quality sequences based on 3 rounds of iterated Phi-BLAST search were kept for further analysis. Multiple-sequence alignment of selected sequences was made to compare the position of variants described in this report with aa located at those positions in different species (Figs. 4 and 5).

D. CYP19A1 Protein Structure Modeling

In silico mutagenesis of the 3-dimensional protein models of CYP19A1, according to the variations identified in the patients, were performed as described earlier [1] using the 3-dimensional x-ray crystal structure of human aromatase (3S79) obtained from the Protein Data Bank database [48]. Model building was performed with programs YASARA [49] and WHATIF [50]. A screening of rotamer libraries was used to minimize stearic clashes with the neighboring residues that resulted from the substitution of aa. Molecular dynamics (MD) simulations were used to optimize the aa side chains. The final model was refined by a 1000 ps MD simulation using the AMBER ff15ipq forcefield [51]. Structure models were drawn using the software Pymol (www.pymol.org), and rendering of images was performed with POVRAY (www.povray.org).

E. Predicting the Effect of Protein Stability Using Site-Directed Mutator

The site-directed mutator (SDM) tool [52] described by Topham and colleagues [53] was used for predicting the effect of *CYP19A1* variants. SDM software uses environment-specific substitution frequencies within homologous protein families to calculate a stability score. The structures of variants used for analysis were generated using the built-in program ANDANTE [54]. SDM provides a pseudo-δ G score for stability prediction and also a potential impact of genetic variants for causing disease.

F. In vitro Functional Testing of CYP19A1 Variants

The human wt *CYP19A1* complementary DNA (cDNA) expression vector was described previously [1]. The new deletion constructs were created according to the cDNA sequences identified by the genetic analysis and minigene experiments. For point mutations, site-directed mutagenesis was performed to obtain the specific cDNA variants. HEK293 cells were transiently transfected with wt and variant CYP19A1 vectors for 48 hours (Lipofectamine 2000). Aromatase activity was then measured by the tritiated water release assay using cold/hot androstenedione as substrate (10 nM/[1β-^{3}H(N)]-androstene-3,17-dione; 20 000 cpm/well) as previously reported [1, 55]. Data represent the mean ± SD of 3 independent experiments performed in duplicate. The student t test was used to test the significance ($P \leq .05$).

G. Tissue Histology Studies

Formalin-embedded tissue biopsy material obtained by laparoscopy of patient 2 (see "Case Reports") was available for histology studies. Tissue was investigated microscopically after hematoxylin and eosin staining. Tissue was compared to ovarian tissues originating from one representative, age-matched normal girl, and one girl with Turner syndrome (TS).

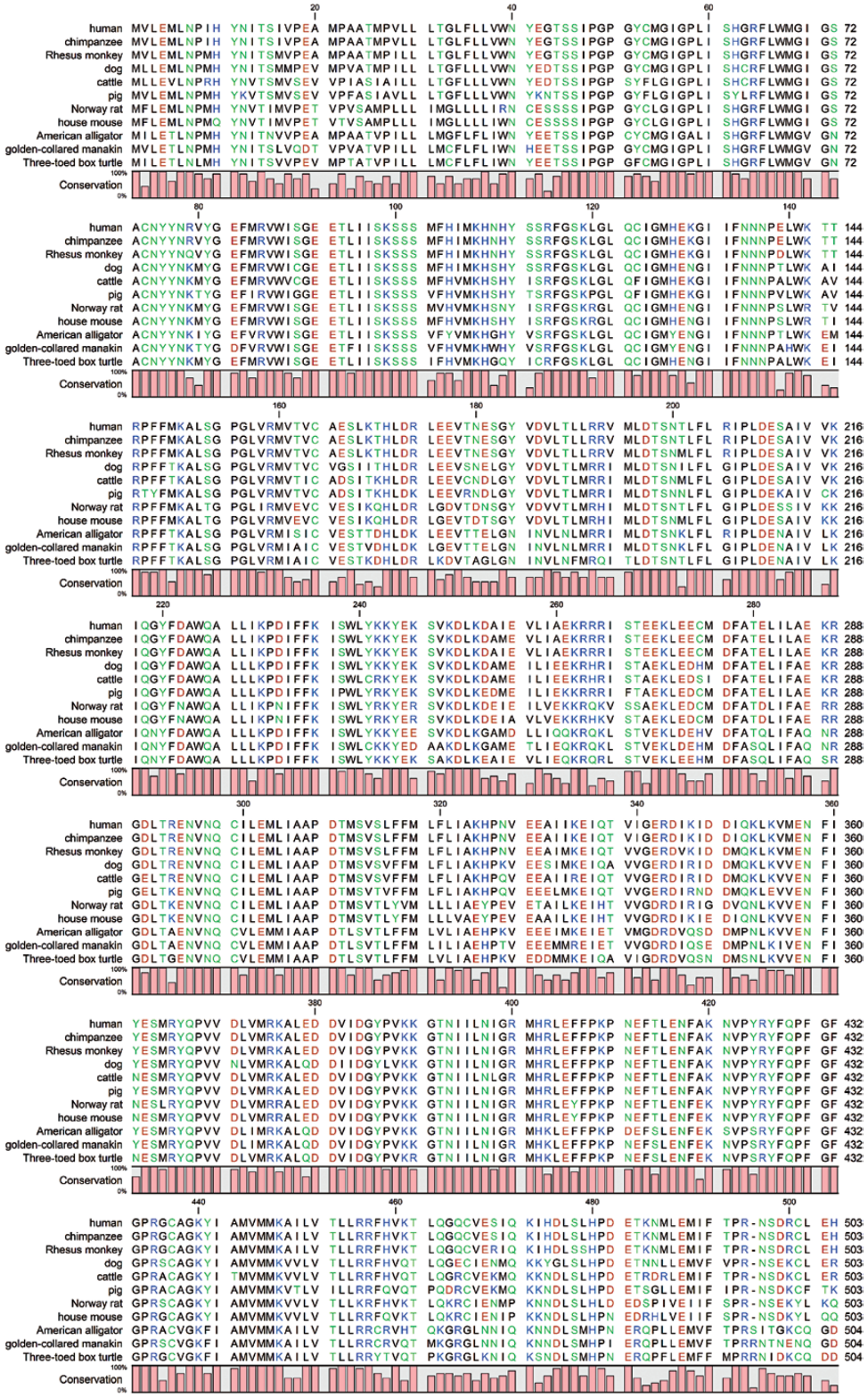

Figure 4. Multiple sequence alignment of affected CYP19A1 amino acid sequences from patients showing that all variants described in this report are conserved in higher primates. The valine 161 residue is well conserved across species and in some cases, a similar amino acid (isoleucine) was found (alligator, manakin, and turtle). The CYP19A1 proteins from human, chimpanzee, rhesus monkey and pig have an arginine at the position 264, whereas dog, cow, and mouse have a histidine, and rat, American alligator, golden-collared manakin, and turtle have glutamine at amino acid position 264. Considering the critical role of arginine 375 in heme binding, it was found to be conserved across species and no substitutions were identified in all the CYP19A1 sequences analyzed.

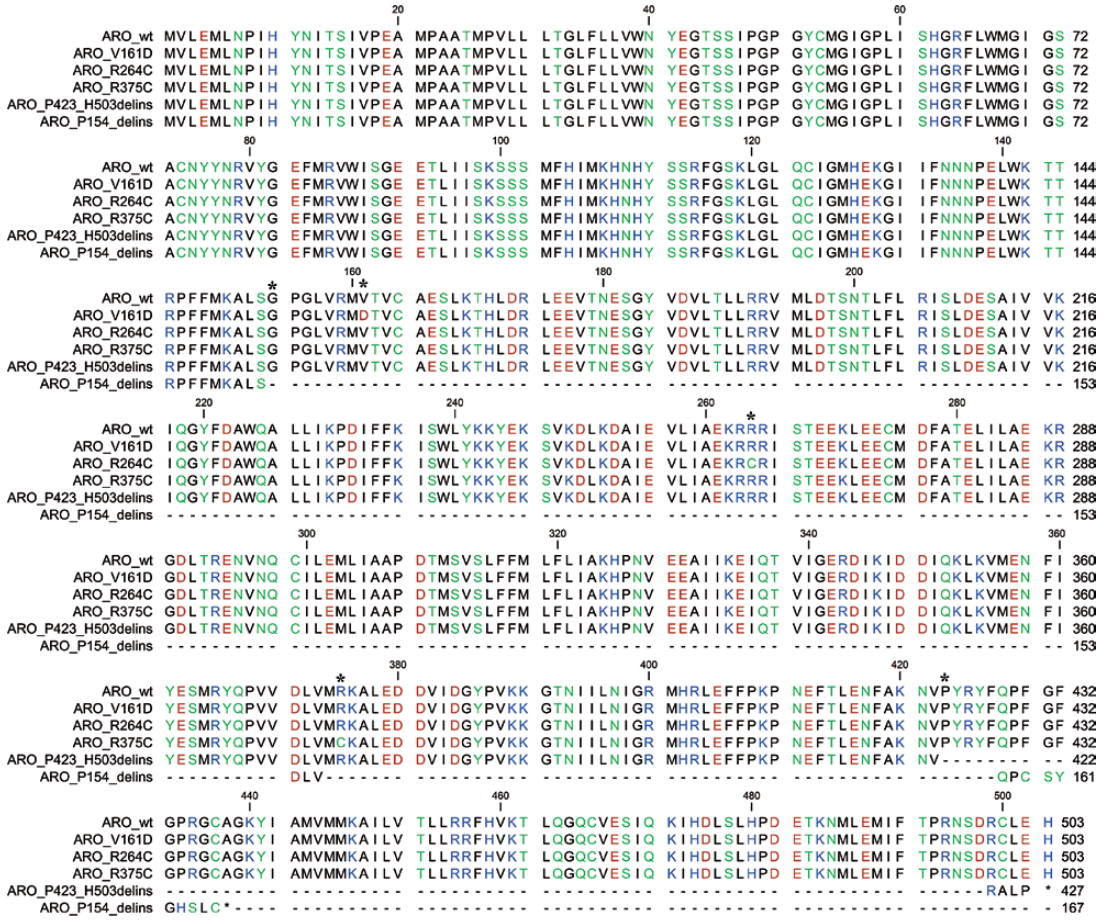

Figure 5. Multiple sequence alignment of CYP19A1 amino acid sequences from patients is shown. All the variants described in this report are conserved in higher primates as shown in Fig. 4.

2. Results

A. Phenotype-Genotype Characterization

We found novel *CYP19A1* variants in 4 girls (Fig. 2) manifesting either at birth with atypical genitalia or puberty with poor breast development, clitoromegaly, abnormal menstrual bleeding, polycystic ovaries, and ovarian torsion (Fig. 3). Three mothers had signs of virilization during pregnancy (Table 2). Biochemical analysis revealed elevated androgens during pregnancy and in the neonate (in family 1), and in the adolescent girls with incomplete pubertal development (patients 3 and 4). Gonadotropins LH and FSH were elevated in the pubertal girls, whereas FSH was also abnormally high in the 3-year-old (Table 2). CAH due to 21-hydroxylase (and PORD) was ruled out by normal serum cortisol and 17-hydroxyprogesterone levels (after adrenocorticotropin stimulation) in all patients, and with urinary steroid profiling on spot urine by gas chromatography–mass spectrometry in patient 2 (data not shown) [56].

Genetic analysis of patient 1 revealed a homozygote splice site deletion at the exon-intron 9-3' boundary (Fig. 2). Both consanguineous parents were heterozygote carriers of this variant. The 4 healthy brothers were not available for analysis. Characterization of this novel variant by minigene experiments revealed that the coded transcript contained the wt *CYP19A1* sequence from exon 2 to exon 9, but then found a stop codon within intron 9 after addition of 6 aa due to the intronic splice site deletion that prevented correct splicing. The

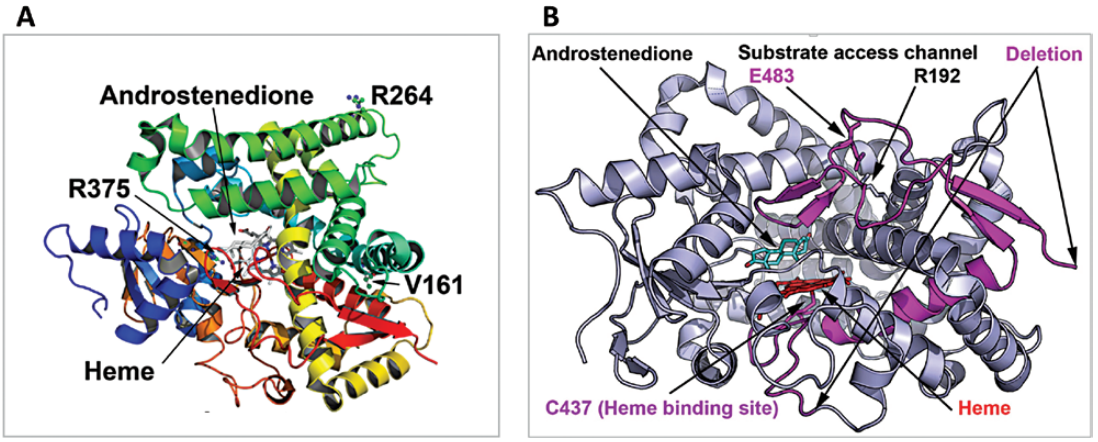

Figure 6. Structural location of CYP19A1 variants. A, Point mutations. Here a ribbons model of CYP19A1 protein colored in the rainbow from amino terminus (violet) to carboxy terminus (red) is shown and the bound substrate, androstenedione, and central heme molecule are depicted as stick models. Heme is ligated to the protein via cysteine 437 residue and forms the catalytic center of the CYP19A1 protein. The substitution of valine 161 for aspartate introduces a buried charge and a hydrophilic residue in the core of the protein, which would cause reduced stability of the structure. The R264 residue on aromatase is surface exposed and located on the G helix of the CYP19A1 structure, which is part of the substrate access channel, and it has been widely reported to be flexible in cytochromes P450. The R375 residue is involved in binding of heme propionate at the catalytic center of the CYP19A1, and its change to cysteine will lead to loss of heme binding and a nonfunctional protein. B, Identified deletion/insertion variations. The P423_H503delins mutation results in loss of critical amino acids in aromatase, including the heme ligating cysteine 437, and would, therefore, result in an inactive enzyme that would also be unstable and subject to degradation.

corresponding protein p.423_503del therefore lacked exon 10 completely and was only 426 aa long compared to 503 aa of the wt protein.

In patient 2, compound heterozygote variants of the *CYP19A1* gene were found. The previously described promoter c.–41C>T variant and a novel deletion/insertion in exon 5 at c.603_608 led to a truncated aromatase protein that was predicted to have no enzyme activity (p.P154_delins) (25). Both parents were carriers of the p.P154_delins variant, and the mother carried, in addition, the c-41C>T variant (Fig. 2). Other family members were phenotypically normal and not available for genetic studies.

Patient 3 had 2 point mutations in exons 5 and 7, corresponding to c.624T>A (p.V161D) and c.932C>T (p.R264C) together with the promoter variant c.–41C>T. The consanguineous parents carried all these variants on 1 allele. Siblings were not affected and were not available for our study.

Finally, a homozygote point mutation in exon 9 was found in patient 4, c.1265C>T, p.R375C. Of the consanguineous parents, only the mother's DNA was available for genetic analysis. She was found to carry the variant on 1 allele (Fig. 2).

B. Bioinformatic Characterization of the CYP19A1 Variants

Multiple-sequence alignment of affected CYP19A1 aa sequences from the patients is shown in Fig. 5. All mutations described in this report are conserved in higher primates (Fig. 4). An analysis of different aromatase sequences across species revealed valine 161 is well conserved across species, and in some cases, a similar aa (isoleucine) was found (alligator, manakin, and turtle). The V161D replacement was predicted to be less stable compared to wt CYP19A1, with a δ G value of –2.5 compared to wt protein. The substitution of valine 161 for an aspartate introduces a buried charge and a hydrophilic residue in the core of the protein, which would cause reduced stability. Further, the helix 144 to 165 is also involved in protein stabilization, and the introduction of a charged residue is likely to cause reduced flexibility (Fig. 6A).

R264C (rs700519) is a common polymorphic variant of CYP19A1 (CYP19A1*4). The R264C variant of CYP19A1 is present at a lower frequency in the European population, with a minor allele frequency (MAF) of 0.02 in the 1000 Genomes database but is more prevalent in the East Asian (MAF 0.17), South East Asian (MAF 0.24) and African (MAF 0.18) populations. The R264 residue on the aromatase is on the surface and located on the G helix of the CYP19A1 structure (Fig. 6A), which is part of the substrate access channel, and it has been widely reported to be flexible in cytochrome P450 proteins. The R264 residue is also the central residue of a 3-arginine cluster that is part of a consensus sequence for several kinases. Therefore, R264 may have a role both in the regulation of substrate access and posttranslational modifications of aromatase. Compared to the R263 position in aromatase, the R264 position is variable among species. The human, chimpanzee, rhesus monkey and pig have an arginine at the position 264; dog, cow, and mouse have a histidine, whereas the rat, American alligator, golden-collared manakin, and turtle have glutamine at position 264. As part of the KRRR sequence (AA 262-265), lysine 262 and arginine 263 are conserved across species and no variations were found at these positions, and at position 265, either arginine or lysine is present across species (Fig. 4).

The R375 residue is involved in binding of heme propionate at the catalytic center of the CYP19A1, and its change to cysteine will lead to loss of heme binding, resulting in a nonfunctional protein, which is consistent with a complete loss of activity observed for this mutation (Figs. 6A and 7). Considering the critical role of arginine 375 in heme binding, it was found to be conserved across species, and no substitutions were identified in all CYP19A1 sequences analyzed (Fig. 4).

The P154delins variant results in a truncated protein, which would be degraded (Fig. 8). The P423_H503delins mutation results in the loss of critical aa in aromatase, including the heme-ligating cysteine 437 (Fig. 6B), and would, therefore, result in an inactive enzyme that would also be unstable and subject to degradation.

C. In vitro Functional Characterization of the Identified CYP19A1 Variants

All *CYP19A1* variants were tested in HEK293 cells for their ability to convert androstenedione to estrone using the tritiated water-release assay, as previously described [1, 57]. Both deletion/insertion variants and the 2 point variants p.V161D and p.R375C showed complete loss of aromatase activity (Fig. 9). By contrast, the p.R264C variation had similar aromatase activity as the wt CYP19A1. The double variant p.V161D and p.R264C, however, showed complete loss of function, like the p.V161D single variant. The functional effect of the promoter variant c.–41C>T on *CYP19A1* expression has been previously described [25].

D. Histological Description of an Aromatase-Deficient Ovary in Infancy

Ovarian tissue for histological evaluation was available from patient 2. At age 3 years, histology showed a normal-appearing ovary with normal-looking stroma and follicles on one side (Fig. 10A) compared to a healthy control ovary of the same age (Fig. 10C). By contrast, on the contralateral side, a streak gonad was identified macroscopically, with histological ovarian-like stroma without follicles (Fig. 10B) as found in typical TS (see age-matched picture of TS in Fig. 10D).

3. Discussion and Conclusion

There are only a few inborn errors of steroidogenesis that cause virilization of 46,XX individuals. The first group of disorders causes not only sex hormone disturbances but also glucocorticoid deficiency, and is therefore called *CAH*. This group comprises 3β-hydroxysteroid dehydrogenase (HSD3B2), 21-hydroxylase (CYP21A2), and 11-hydroxylase (CYP11B1) deficiencies. The second group with normal glucocorticoid production comprises aromatase deficiency (CYP19A1) and PORD, although in PORD stimulated cortisol production

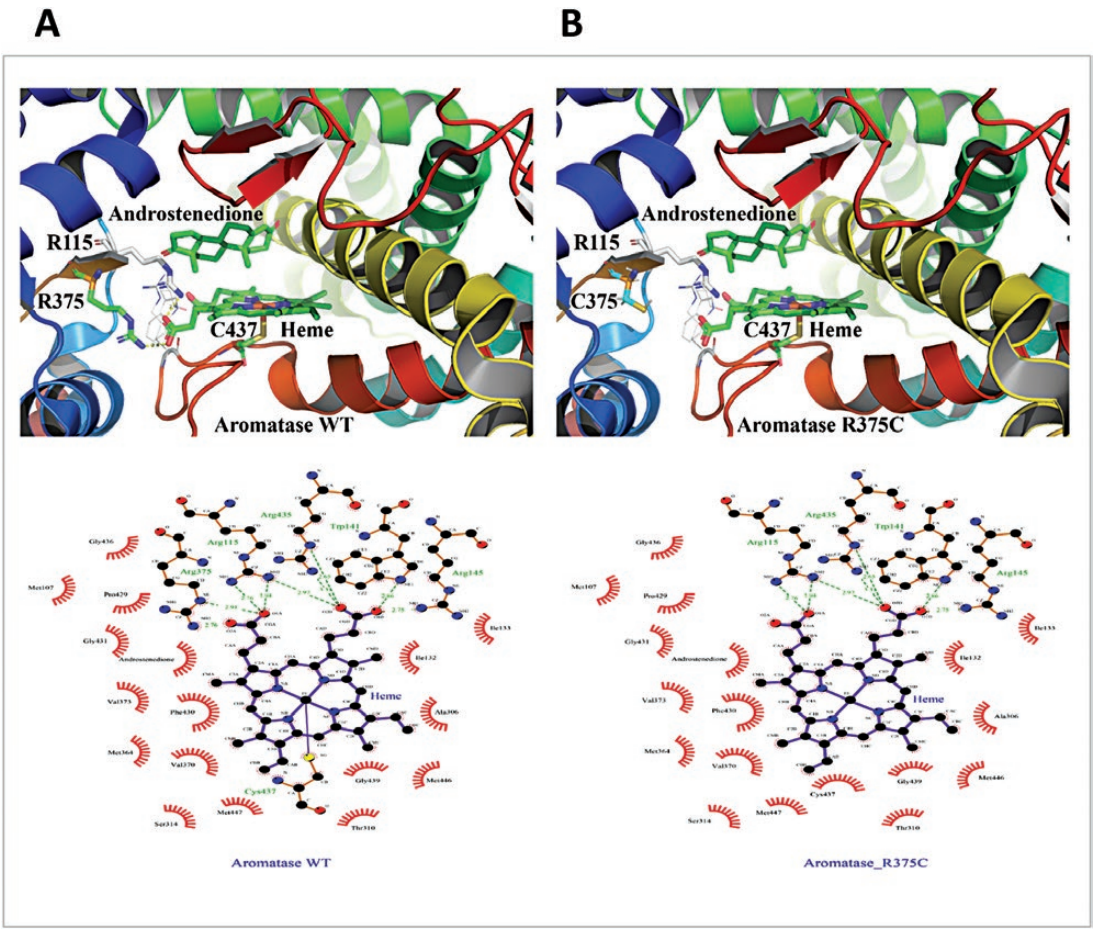

Figure 7. Critical role of arginine 375 in heme binding. A and B, Structures of A, wild-type (WT), and B, R375C aromatase, shown as a ribbons model. The R375 residue is essential for the binding of heme at the catalytic center of the A, CYP19A1, and its change to B, cysteine, will lead to loss of heme binding, resulting in a nonfunctional protein. A complete loss of activity was observed for the R375C variant. Therefore, the arginine 375 residue has a critical role in heme binding and activity of aromatase. These observations are further substantiated by the conservation of R375 residue in aromatase across species, and no substitutions were identified in all CYP19A1 sequences analyzed (Fig. 4). C and D, A close-up of heme ligation in aromatase C, WT and D, R375C. D, After the change of arginine 375 to cysteine, one of the bonds holding the heme in place, formed between the propionate group in heme and arginine 375, is disrupted. The heme in aromatase, similar to other cytochrome P450 proteins, is held together by several bonds between the propionates of heme and arginines or histidine/tryptophan groups located at the catalytic center. Disruption of these linkages will lead to an unstable heme-binding site in aromatase and loss of heme, which would cause a nonfunctional protein. All the critical arginines (115, 145, and 375), as well as tryptophan 141 and cysteine 427, are conserved across species (Fig. 4), and no variation is observed at any of these places, confirming the importance of these amino acids in the function of aromatase.

is often also compromised [56, 58]. Furthermore, mothers virilize during pregnancy only with disorders of the second group, which affect the aromatization of fetal androgens by the fetal-placental unit.

All girls with CYP19A1 deficiency reported in this study had normal cortisol production but suffered from androgen excess that manifested in utero (in 3 out of 4), at birth (in 2 to 3 out of 4), or puberty (in 1 or 2 out of 4) (see Table 2). Whether a detailed examination of the external genitalia would have revealed some atypical findings in patient 3 at birth remains speculative. So far, most reported 46,XX individuals with aromatase deficiency manifested at birth with moderate to severe virilization of the external genitalia

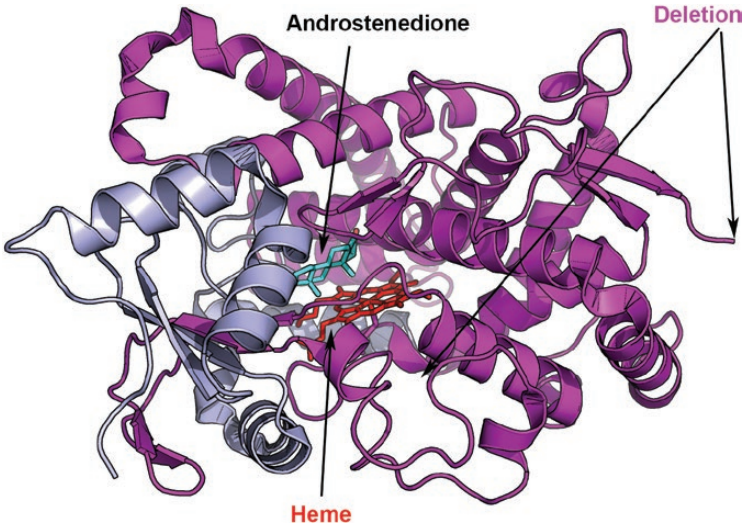

Figure 8. The P154delIns protein variant lacks most of the critical residues of aromatase required for catalytic function because of truncation (shown in magenta). Such a small protein, without functionally important structural features, will be misfolded and degraded, leading to a complete loss of aromatase activity.

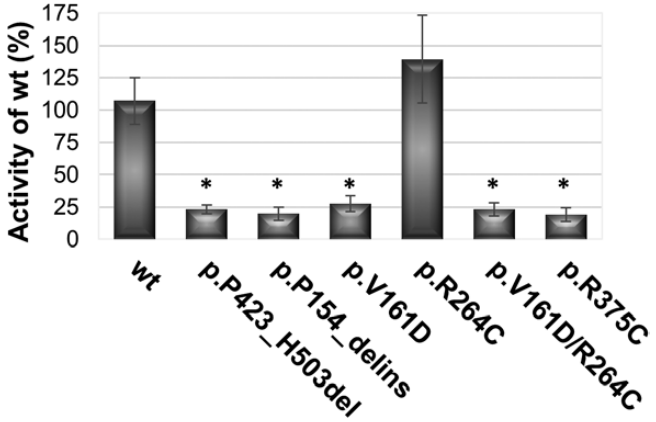

Figure 9. Aromatase activity of identified *CYP19A1* variants. Variants were built into the mammalian expression vector containing wt *CYP19A1* cDNA. HEK293 cells were transiently transfected with wt and variant CYP19A1 plasmids, and aromatase activity was assessed by the tritiated water-release assay testing conversion of androstenedione to estrone. Compared to wt, all variants except p.R264C showed complete loss of activity. **P* value is less than or equal to .05.

(Prader III-V) (n = 25/34; Table 1). This has led to male sex assignment at birth in three 46,XX individuals, 2 of whom were reassigned to the female sex after diagnosis in childhood. Signs of virilization during pregnancy have been described in about half of mothers carrying an affected child. During infancy and childhood, ovarian cysts were noted in several and were either symptomatic or seen by imaging studies. At puberty, incomplete development with poor breast development, menstrual cycle anomalies, polycystic ovaries, and signs of androgen excess (eg, hirsutism, acne, enlarged clitoris) are typically due to estrogen deficiency and elevated androgens. Late diagnosis at pubertal age is described in less than one-third of reported 46,XX aromatase-deficient female patients. Of the 15 reported female individuals older than pubertal age, 4 showed no signs of spontaneous puberty, 6 had incomplete development, and only 5 spontaneously reached Tanner 5 (Table 1).

By contrast, affected 46,XY individuals typically present at around age 20 to 30 years with extremely tall stature due to failure of growth arrest. Only if the diagnosis is known in the family or maternal virilization during pregnancy raised suspicion, may diagnosis be

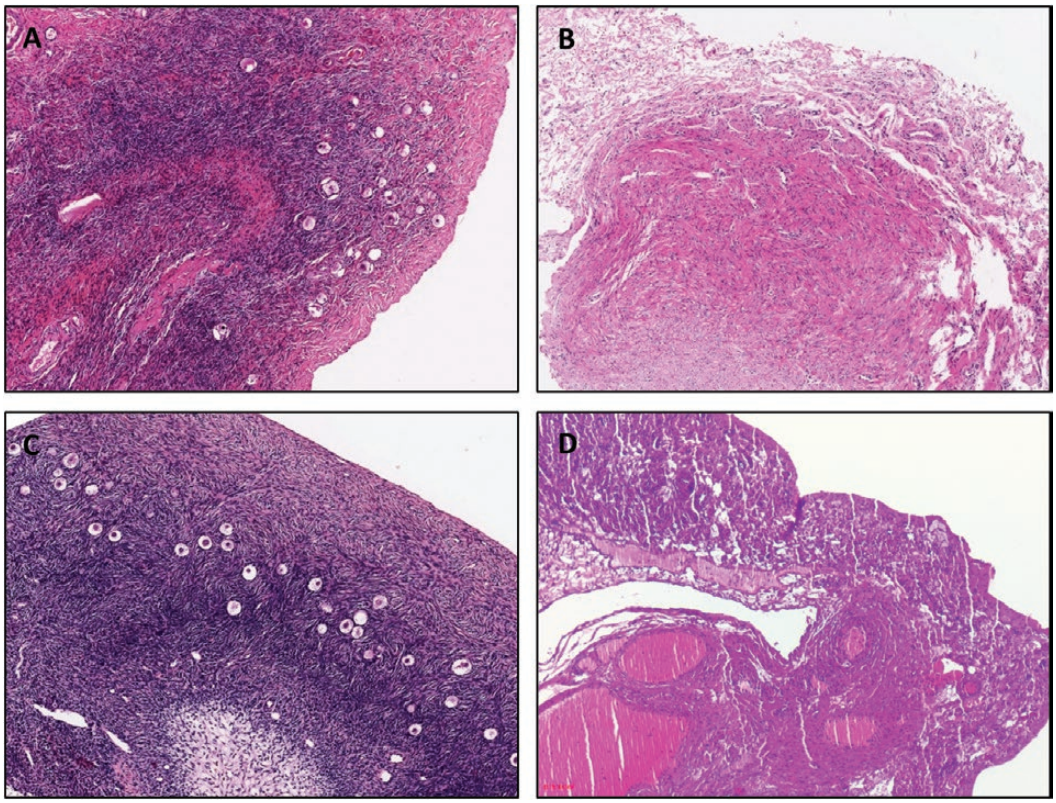

Figure 10. Histology of an ovary originating from a toddler with aromatase deficiency. A, Hematoxylin and eosin (HE) histology picture of one ovary of patient 2 showing a normal ovary with normal stroma and follicles. B, HE histology of the contralateral ovary showing a streak gonad without follicles. C, HE picture of a normal, age-matched ovary. D, HE picture of a typical Turner syndrome streak ovary, age matched.

made earlier in boys. We also suspect that the diagnosis is less often made in boys than girls because the clinical picture is less remarkable and manifests only in early adulthood when genetic disorders are less suspected; this may be evidenced by fewer reported cases of male patients in the literature (n = 13/47; Table 1), which does not reflect the autosomal recessive inheritance and the true incidence.

Owing to enlarged ovaries with cysts or polycystic ovaries, torsion of an ovary is a frequent complication that may occur early in life. This complication can be prevented by very low-dose estrogen replacement starting early in life [34, 59]. At puberty, sex hormone replacement therapy is required to allow for complete pubertal development and normal menstrual bleeding. So far no successful pregnancy has been described in a woman with aromatase deficiency. However, it is not excluded that this could be possible with the help of assisted reproduction, as recently demonstrated in a woman with 17-hydroxylase (CYP17A1) deficiency, a steroid enzyme essential for the production of all sex hormones [60]. Histologic investigations of ovarian tissue of female patients carrying *CYP19A1* variants are scarce. We had a chance to investigate ovarian biopsy material in patient 2 and found a normal-looking ovary on one side and a streak gonad on the other. In the literature, ovaries are often reported to look normal or only slightly abnormal in size by imaging studies in very young girls, although smaller cysts may be found very early when specifically searched for. Imaging studies later during infancy and childhood mostly reveal abnormal ovarian cysts, which may resemble the picture of a polycystic ovary by the age of puberty (Table 1). This resulted in ovarian torsion in several cases, even at a very young age.

Furthermore, streak ovaries or absent/nonvisualized ovaries have been reported with *CYP19A1* deficiency [17, 27, 30]. Thus it appears that aromatase deficiency might lead

to an earlier destruction of the ovary than with other steroid biosynthetic disorders such as lipoid CAH due to steroidogenic acute regulatory protein deficiency. In STAR deficiency, lipid overload destroys the gonad over time and a PCOS-like phenotype is not characteristic [61]. Studies of ovary development have shown that concerted activity of aromatase (as well as other steroidogenic enzymes such as HSD17s and HSD3B2), steroid hormones (eg, estrogens and progesterone), and gonadotropins (eg, FSH) is essential for normal primordial follicle pool development during fetal life as well as for normal follicle maturation and ovulation in the adult ovary [62]. In the human fetal ovaries, expression of aromatase and estrogen receptors is upregulated in the second trimester when primordial folliculogenesis is fully active [63]. By contrast, mice lacking aromatase activity develop ovaries with diminished oocyte density [64, 65]. In addition, coordinated action of estrogens and FSH are also crucial for the proper timing of folliculogenesis [66]. In aromatase deficiency lack of estrogens results in abnormal gonadotropin feedback, which affects follicle growth in the ovaries. It has been shown that for the formation of (poly-)cystic ovaries elevated FSH plays a critical role [67, 68]. Overall, these facts from the literature may explain the ovarian phenotypes (both streak gonads and polycystic ovaries) seen with aromatase deficiency. Based on this knowledge and clinical experience (eg, [34]) (preventive) treatment of polycystic ovaries with estrogen replacement normalizing FSH should be advised in all patients with aromatase deficiency.

Human *CYP19A1* variants described so far are summarized in Table 1. They span over all exons and comprise all types of genetic variations, as shown in Fig. 1. The genotype-phenotype correlation seems doubtful, but structure-function prediction has revealed consistent results with few exceptions. We found novel *CYP19A1* variants in 4 affected girls. These variants were all predicted to severely affect enzyme activity, and functional tests confirmed this prediction. Novel deletion-insertion variants of *CYP19A1* found in patients 1 and 2 received the label "pathogenic" when characterized according to American College of Medical Genetics and Genomics (ACMG) standards and guidelines [69]. *In silico* structure-function studies of the identified *CYP19A1* variations showed loss of the heme-binding site due to the *R375C* variation and was predicted to cause a loss of function. In the case of the *V161D* variant, a loss of protein stability leading to degradation was predicted. This novel point mutation found in patient and family 3 is likely pathogenic according to ACMG characterization and was found in combination with known variants –41C>T and *R264C*. Variants *R264C* and *R375C* have been described previously [18, 70]. In line with our results, *R375C* was found to cause a complete loss of function. Although *in silico* structural prediction could not provide a clear analysis for the *R264C* variant, we found that the *R264C* variant showed activity similar to wt *CYP19A1*. The *R264C* variation is known in the literature as a polymorphism of *CYP19A1*, which seems common in Southeast Asia [70]. However, this *CYP19A1* variant may affect enzyme function when it is present in combination with specific variants of cytochrome P450 oxidoreductase (*POR*), as reported in a recent study [70]. Partial loss of function of aromatase activity has been found with *CYP19A1* variant *R192H* [1] and with several *POR* variants [56, 71-73]. Patients carrying these mutations manifest with variable degrees of virilization either at birth or puberty.

In summary, we describe clinical, genetic, and functional implications of novel *CYP19A1* variants identified in 4 girls originating from Africa and India. CYP19A1 deficiency seems to cause maternal virilization in more than 50% of pregnancies and manifest with some degree of ambiguous genitalia in more than 70% of 46,XX newborns. Additionally, about 80% of affected girls are unable to enter or complete puberty spontaneously and need hormonal replacement therapies. The ovary with aromatase deficiency develops a polycystic ovary phenotype in most cases, but streak gonads are also seen. Normal aromatase activity in concerted action with other steroid enzymes and hormones as well as gonadotropins seem essential for proper ovarian follicle pool development during fetal life and for follicle maturation and ovulation during the reproductive years.

Acknowledgments

Financial Support: This work was supported in part by a grant from the Swiss National Science Foundation (SNF 320030-146127 to C.E.F.).

Additional Information

Correspondence: Christa E. Flück, MD, Pediatric Endocrinology and Diabetology, University Children's Hospital Bern, Freiburgstrasse 15 – C845, 3010 Bern, Switzerland. E-mail: christa.flueck@dbmr.unibe.ch.

Disclosure Summary: The authors have nothing to disclose.

Data Availability: The data sets generated and analyzed during the present study are not publicly available but are available from the corresponding author on reasonable request. Restrictions apply to the availability of data generated or analyzed during this study to preserve patient confidentiality or because they were used under license. The corresponding author will on request detail the restrictions and any conditions under which access to some data may be provided.

References

1. Bouchoucha N, Samara-Boustani D, Pandey AV, et al. Characterization of a novel CYP19A1 (aromatase) R192H mutation causing virilization of a 46,XX newborn, undervirilization of the 46,XY brother, but no virilization of the mother during pregnancies. *Mol Cell Endocrinol.* 2014;**390**(1-2):8–17.
2. Grumbach MM, Auchus RJ. Estrogen: consequences and implications of human mutations in synthesis and action. *J Clin Endocrinol Metab.* 1999;**84**(12):4677–4694.
3. Simpson ER, Mahendroo MS, Means GD, et al. Aromatase cytochrome P450, the enzyme responsible for estrogen biosynthesis. *Endocr Rev.* 1994;**15**(3):342–355.
4. Stocco C. Tissue physiology and pathology of aromatase. *Steroids.* 2012;**77**(1-2):27–35.
5. Di Nardo G, Gilardi G. Human aromatase: perspectives in biochemistry and biotechnology. *Biotechnol Appl Biochem.* 2013;**60**(1):92–101.
6. Neunzig J, Milhim M, Schiffer L, et al. The steroid metabolite 16(β)-OH-androstenedione generated by CYP21A2 serves as a substrate for CYP19A1. *J Steroid Biochem Mol Biol.* 2017;**167**:182–191.
7. Shozu M, Akasofu K, Harada T, Kubota Y. A new cause of female pseudohermaphroditism: placental aromatase deficiency. *J Clin Endocrinol Metab.* 1991;**72**(3):560–566.
8. Richter-Unruh. Aromatase deficiency: delayed puberty in a German girl is due to 2 new mutations of the CYP19 gene. Paper presented at: 90th Annual Meeting of the Endocrine Society; June 2008, San Francisco, CA. Abstr P2-590.
9. Ozen S, Atik T, Korkmaz O, et al. Aromatase deficiency in two siblings with 46, XX karyotype raised as different genders: a novel mutation (p.R115X) in *CYP19A1* gene [Published online ahead of print April 10, 2019]. *J Clin Res Pediatr Endocrinol.* Doi:10.4274/jcrpe.galenos.2019.2018.0198.
10. Ludwikowski B, Heger S, Datz N, Richter-Unruh A, González R. Aromatase deficiency: rare cause of virilization. *Eur J Pediatr Surg.* 2013;**23**(5):418–422.
11. Marino R, Perez Garrido N, Costanzo M, et al. Five new cases of 46,XX aromatase deficiency: clinical follow-up from birth to puberty, a novel mutation, and a founder effect. *J Clin Endocrinol Metab.* 2015;**100**(2):E301–E307.
12. Maffei L, Murata Y, Rochira V, et al. Dysmetabolic syndrome in a man with a novel mutation of the aromatase gene: effects of testosterone, alendronate, and estradiol treatment. *J Clin Endocrinol Metab.* 2004;**89**(1):61–70.
13. Belgorosky A, Pepe C, Marino R, et al. Hypothalamic-pituitary-ovarian axis during infancy, early and late prepuberty in an aromatase-deficient girl who is a compound heterocygote for two new point mutations of the *CYP19* gene. *J Clin Endocrinol Metab.* 2003;**88**(11):5127–5131.
14. Pepe CM, Saraco NI, Baquedano MS, et al. The cytochrome P450 aromatase lacking exon 5 is associated with a phenotype of nonclassic aromatase deficiency and is also present in normal human steroidogenic tissues. *Clin Endocrinol (Oxf).* 2007;**67**(5):698–705.
15. Guercio G, Di Palma MI, Pepe C, et al. Metformin, estrogen replacement therapy and gonadotropin inhibition fail to improve insulin sensitivity in a girl with aromatase deficiency. *Horm Res.* 2009;**72**(6):370–376.
16. Carani C, Qin K, Simoni M, et al. Effect of testosterone and estradiol in a man with aromatase deficiency. *N Engl J Med.* 1997;**337**(2):91–95.

17. Ludwig M, Beck A, Wickert L, et al. Female pseudohermaphroditism associated with a novel homozygous G-to-A (V370-to-M) substitution in the P-450 aromatase gene. *J Pediatr Endocrinol Metab*. 1998;**11**(5):657–664.
18. Morishima A, Grumbach MM, Simpson ER, Fisher C, Qin K. Aromatase deficiency in male and female siblings caused by a novel mutation and the physiological role of estrogens. *J Clin Endocrinol Metab*. 1995;**80**(12):3689–3698.
19. Baykan EK, Erdoğan M, Özen S, Darcan Ş, Saygılı LF. Aromatase deficiency, a rare syndrome: case report. *J Clin Res Pediatr Endocrinol*. 2013;**5**(2):129–132.
20. Maffei L, Rochira V, Zirilli L, et al. A novel compound heterozygous mutation of the aromatase gene in an adult man: reinforced evidence on the relationship between congenital oestrogen deficiency, adiposity and the metabolic syndrome. *Clin Endocrinol (Oxf)*. 2007;**67**(2):218–224.
21. Lin L, Ercan O, Raza J, et al. Variable phenotypes associated with aromatase (CYP19) insufficiency in humans. *J Clin Endocrinol Metab*. 2007;**92**(3):982–990.
22. Ito Y, Fisher CR, Conte FA, Grumbach MM, Simpson ER. Molecular basis of aromatase deficiency in an adult female with sexual infantilism and polycystic ovaries. *Proc Natl Acad Sci U S A*. 1993;**90**(24):11673–11677.
23. Conte FA, Grumbach MM, Ito Y, Fisher CR, Simpson ER. A syndrome of female pseudohermaphrodism, hypergonadotropic hypogonadism, and multicystic ovaries associated with missense mutations in the gene encoding aromatase (P450arom). *J Clin Endocrinol Metab*. 1994;**78**(6):1287–1292.
24. Chen Z, Wang O, Nie M, et al. Aromatase deficiency in a Chinese adult man caused by novel compound heterozygous *CYP19A1* mutations: effects of estrogen replacement therapy on the bone, lipid, liver and glucose metabolism. *Mol Cell Endocrinol*. 2015;**399**:32–42.
25. Hauri-Hohl A, Meyer-Böni M, Lang-Muritano M, Hauri-Hohl M, Schoenle EJ, Biason-Lauber A. Aromatase deficiency owing to a functional variant in the placenta promoter and a novel missense mutation in the *CYP19A1* gene. *Clin Endocrinol (Oxf)*. 2011;**75**(1):39–43.
26. Dursun F, Ceylaner S. A novel homozygous *CYP19A1* gene mutation: aromatase deficiency mimicking congenital adrenal hyperplasia in an infant without obvious maternal virilisation. *J Clin Res Pediatr Endocrinol*. 2019;**11**(2):196–201.
27. Mazen I, McElreavey K, Elaidy A, Kamel AK, Abdel-Hamid MS. Aromatase deficiency due to a homozygous *CYP19A1* mutation in a 46,XX Egyptian patient with ambiguous genitalia. *Sex Dev*. 2017;**11**(5-6):275–279.
28. Deladoëy J, Flück C, Bex M, Yoshimura N, Harada N, Mullis PE. Aromatase deficiency caused by a novel P450arom gene mutation: impact of absent estrogen production on serum gonadotropin concentration in a boy. *J Clin Endocrinol Metab*. 1999;**84**(11):4050–4054.
29. Zhu WJ, Cheng T, Zhu H, et al. Aromatase deficiency: a novel compound heterozygous mutation identified in a Chinese girl with severe phenotype and obvious maternal virilization. *Mol Cell Endocrinol*. 2016;**433**:66–74.
30. Gagliardi L, Scott HS, Feng J, Torpy DJ. A case of aromatase deficiency due to a novel *CYP19A1* mutation. *BMC Endocr Disord*. 2014;**14**:16.
31. Saraco N, Nesi-Franca S, Sainz R, et al. An intron 9 *CYP19* gene variant (IVS9 + 5G>A), present in an aromatase-deficient girl, affects normal splicing and is also present in normal human steroidogenic tissues. *Horm Res Paediatr*. 2015;**84**(4):275–282.
32. Harada N, Ogawa H, Shozu M, et al. Biochemical and molecular genetic analyses on placental aromatase (P-450AROM) deficiency. *J Biol Chem*. 1992;**267**(7):4781–4785.
33. Mullis PE, Yoshimura N, Kuhlmann B, Lippuner K, Jaeger P, Harada H. Aromatase deficiency in a female who is compound heterozygote for two new point mutations in the P450arom gene: impact of estrogens on hypergonadotropic hypogonadism, multicystic ovaries, and bone densitometry in childhood. *J Clin Endocrinol Metab*. 1997;**82**(6):1739–1745.
34. Janner M, Flück CE, Mullis PE. Impact of estrogen replacement throughout childhood on growth, pituitary-gonadal axis and bone in a 46,XX patient with *CYP19A1* deficiency. *Horm Res Paediatr*. 2012;**78**(4):261–268.
35. Bouillon R, Bex M, Vanderschueren D, Boonen S. Estrogens are essential for male pubertal periosteal bone expansion. *J Clin Endocrinol Metab*. 2004;**89**(12):6025–6029.
36. Herrmann BL, Saller B, Janssen OE, et al. Impact of estrogen replacement therapy in a male with congenital aromatase deficiency caused by a novel mutation in the *CYP19* gene. *J Clin Endocrinol Metab*. 2002;**87**(12):5476–5484.
37. Lanfranco F, Zirilli L, Baldi M, et al. A novel mutation in the human aromatase gene: insights on the relationship among serum estradiol, longitudinal growth and bone mineral density in an adult man under estrogen replacement treatment. *Bone*. 2008;**43**(3):628–635.

38. Unal E, Yıldırım R, Taş FF, Demir V, Onay H, Haspolat YK. Aromatase deficiency due to a novel mutation in CYP19A1 gene. *J Clin Res Pediatr Endocrinol*. 2018;**10**(4):377–381.
39. Mittre Hervé MH, Kottler ML, Pura M. Human gene mutations. Gene symbol: *CYP19*. Disease: aromatase deficiency. *Hum Genet*. 2004;**114**(2):224.
40. Akçurin S, Türkkahraman D, Kim WY, Durmaz E, Shin JG, Lee SJ. A novel null mutation in P450 aromatase gene (*CYP19A1*) associated with development of hypoplastic ovaries in humans. *J Clin Res Pediatr Endocrinol*. 2016;**8**(2):205–210.
41. Abstracts of the 51st Annual Meeting of the European Society for Paediatric Endocrinology (ESPE). Leipzig, Germany. September 20–23, 2012. *Horm Res Paediatr*. 2012;**78**(Suppl.1):1–349.
42. Portrat-Doyen SFM, Forest MG, Nicolino M, Morel Y, Chatelain PC. Female pseudohermaphroditism (FHP) resulting from aromatase(P40arom) deficiency associated with a novel mutation R457X in the *CYP19* gene. *Horm Res*. 1996;**46**(Suppl 2):14.
43. Bulun SE. Clinical review 78: aromatase deficiency in women and men: would you have predicted the phenotypes? *J Clin Endocrinol Metab*. 1996;**81**(3):867–871.
44. Shozu M, Sebastian S, Takayama K, et al. Estrogen excess associated with novel gain-of-function mutations affecting the aromatase gene. *N Engl J Med*. 2003;**348**(19):1855–1865.
45. Stratakis CA, Vottero A, Brodie A, et al. The aromatase excess syndrome is associated with feminization of both sexes and autosomal dominant transmission of aberrant P450 aromatase gene transcription. *J Clin Endocrinol Metab*. 1998;**83**(4):1348–1357.
46. Ashkenazy H, Erez E, Martz E, Pupko T, Ben-Tal N. ConSurf 2010: calculating evolutionary conservation in sequence and structure of proteins and nucleic acids. *Nucleic Acids Res*. 2010;**38**(Web Server issue):W529–W533.
47. Glaser F, Pupko T, Paz I, et al. ConSurf: identification of functional regions in proteins by surface-mapping of phylogenetic information. *Bioinformatics*. 2003;**19**(1):163–164.
48. Ghosh D, Lo J, Morton D, et al. Novel aromatase inhibitors by structure-guided design. *J Med Chem*. 2012;**55**(19):8464–8476.
49. Krieger E, Darden T, Nabuurs SB, Finkelstein A, Vriend G. Making optimal use of empirical energy functions: force-field parameterization in crystal space. *Proteins*. 2004;**57**(4):678–683.
50. Vriend G. WHAT IF: a molecular modeling and drug design program. *J Mol Graph*. 1990;**8**(1):52–6, 29.
51. Debiec KT, Cerutti DS, Baker LR, Gronenborn AM, Case DA, Chong LT. Further along the road less traveled: AMBER ff15ipq, an original protein force field built on a self-consistent physical model. *J Chem Theory Comput*. 2016;**12**(8):3926–3947.
52. Worth CL, Bickerton GR, Schreyer A, et al. A structural bioinformatics approach to the analysis of nonsynonymous single nucleotide polymorphisms (nsSNPs) and their relation to disease. *J Bioinform Comput Biol*. 2007;**5**(6):1297–1318.
53. Topham CM, Srinivasan N, Blundell TL. Prediction of the stability of protein mutants based on structural environment-dependent amino acid substitution and propensity tables. *Protein Eng*. 1997;**10**(1):7–21.
54. Smith RE, Lovell SC, Burke DF, Montalvao RW, Blundell TL. Andante: reducing side-chain rotamer search space during comparative modeling using environment-specific substitution probabilities. *Bioinformatics*. 2007;**23**(9):1099–1105.
55. Pandey AV, Kempná P, Hofer G, Mullis PE, Flück CE. Modulation of human CYP19A1 activity by mutant NADPH P450 oxidoreductase. *Mol Endocrinol*. 2007;**21**(10):2579–2595.
56. Pandey AV, Flück CE. NADPH P450 oxidoreductase: structure, function, and pathology of diseases. *Pharmacol Ther*. 2013;**138**(2):229–254.
57. Lephart ED, Simpson ER. Assay of aromatase activity. *Methods Enzymol*. 1991;**206**:477–483.
58. Parween S, Fernández-Cancio M, Benito-Sanz S, et al. Molecular basis of CYP19A1 deficiency in a 46, XX patient with R550W mutation in POR: expanding the PORD phenotype [Published online ahead of print February 15, 2020]. *J Clin Endocrinol Metab*. Doi:10.1210/clinem/dgaa076
59. Burckhardt MA, Obmann V, Wolf R, Janner M, Flück CE, Mullis PE. Ovarian and uterine development and hormonal feedback mechanism in a 46 XX patient with CYP19A1 deficiency under low dose estrogen replacement. *Gynecol Endocrinol*. 2015;**31**(5):349–354.
60. Bianchi PH, Gouveia GR, Costa EM, et al. Successful live birth in a woman with 17α-hydroxylase deficiency through IVF frozen-thawed embryo transfer. *J Clin Endocrinol Metab*. 2016;**101**(2):345–348.
61. Bose HS, Pescovitz OH, Miller WL. Spontaneous feminization in a 46,XX female patient with congenital lipoid adrenal hyperplasia due to a homozygous frameshift mutation in the steroidogenic acute regulatory protein. *J Clin Endocrinol Metab*. 1997;**82**(5):1511–1515.

62. Grive KJ, Freiman RN. The developmental origins of the mammalian ovarian reserve. *Development*. 2015;**142**(15):2554–2563.
63. Fowler PA, Anderson RA, Saunders PT, et al. Development of steroid signaling pathways during primordial follicle formation in the human fetal ovary. *J Clin Endocrinol Metab*. 2011;**96**(6):1754–1762.
64. Britt KL, Saunders PK, McPherson SJ, Misso ML, Simpson ER, Findlay JK. Estrogen actions on follicle formation and early follicle development. *Biol Reprod*. 2004;**71**(5):1712–1723.
65. Dutta S, Mark-Kappeler CJ, Hoyer PB, Pepling ME. The steroid hormone environment during primordial follicle formation in perinatal mouse ovaries. *Biol Reprod*. 2014;**91**(3):68.
66. Wang C, Zhou B, Xia G. Mechanisms controlling germline cyst breakdown and primordial follicle formation. *Cell Mol Life Sci*. 2017;**74**(14):2547–2566.
67. Kumar TR, Wang Y, Lu N, Matzuk MM. Follicle stimulating hormone is required for ovarian follicle maturation but not male fertility. *Nat Genet*. 1997;**15**(2):201–204.
68. Themmen APN, Huhtaniemi IT. Mutations of gonadotropins and gonadotropin receptors: elucidating the physiology and pathophysiology of pituitary-gonadal function. *Endocr Rev*. 2000;**21**(5):551–583.
69. Richards S, Aziz N, Bale S, et al; ACMG Laboratory Quality Assurance Committee. Standards and guidelines for the interpretation of sequence variants: a joint consensus recommendation of the American College of Medical Genetics and Genomics and the Association for Molecular Pathology. *Genet Med*. 2015;**17**(5):405–424.
70. Parween S, DiNardo G, Baj F, Zhang C, Gilardi G, Pandey AV. Differential effects of variations in human P450 oxidoreductase on the aromatase activity of *CYP19A1* polymorphisms R264C and R264H. *J Steroid Biochem Mol Biol*. 2020;**196**:105507.
71. Flück CE, Pandey AV. Impact on CYP19A1 activity by mutations in NADPH cytochrome P450 oxidoreductase. *J Steroid Biochem Mol Biol*. 2017;**165**(Pt A):64–70.
72. Flück CE, Mallet D, Hofer G, et al. Deletion of P399_E401 in NADPH cytochrome P450 oxidoreductase results in partial mixed oxidase deficiency. *Biochem Biophys Res Commun*. 2011;**412**(4):572–577.
73. Udhane SS, Parween S, Kagawa N, Pandey AV. Altered CYP19A1 and CYP3A4 activities due to mutations A115V, T142A, Q153R and P284L in the human P450 oxidoreductase. *Front Pharmacol*. 2017;**8**:580.